Cancer Therapy with Heavy Particles

F. Rosalbino

Dipartimento di Scienza Applicata e Tecnologia (DISAT) – Politecnico di Torino – Italy

Abstract

Conventional radiotherapy techniques for the treatment of malignant tumors are known to carry some risk as a method of combatting cancerous cells. The damage caused to healthy tissue as a part of these treatments poses a significant obstacle to overcome in the fields of radiobiology and oncology. The use of linear particle accelerators and cyclotrons to generate beams of charged radioactive particles for use in cancer therapy has been developed over recent years, and new and more effective cancer treatments such as hadron therapy have been made possible because of experimental particle physics and hold the promise of greater survival rates for patients. The effectivity of such particle physics based treatments is discussed here, and potential new treatments explored.

Keywords: antiprotons, particle therapy, hadron therapy, radiobiology

1. Introduction

Standard radiotherapy is carried out in hospitals as a means of combatting cancerous cells. This treatment consists of using ionizing radiation to damage the DNA of the targeted cells, rendering the cells unable to reproduce. The radiation ionizes molecules in the cells, creating free radical compounds that attack and damage DNA. In order to replicate itself, the cell must repair the damage done to the DNA. Many tumors and cancerous cells possess a greatly reduced ability to repair their damaged DNA compared to normal, healthy cells. This then allows for an enhanced tumor control method, such as chemotherapy or surgery to destroy the tumor [1].

Radiation is highly effective in killing tumor cells, but this effectivity can, and often does, come at the cost of damage to the surrounding tissue. Tissues comprised of fast-dividing cells, such as skin, mucosal linings, and bone marrow, are extremely susceptible to the damaging effects of radiation. Diarrhea, nausea, and vomiting are common side effects in patients who receive radiation therapy to any organs in proximity to the gastrointestinal tract [1]. In the case of whole-body irradiation, the lymphocytes in the blood can be damaged as much as the intended cancerous cells, and the immune system can be suppressed, leading to dangerous secondary infections [1].

The most common form radiotherapy involves the bombardment of the tumor with high energy photons, typically in the MeV range. These photons are usually either X-rays created *in situ,* or gamma rays (γ-rays) from a radioactive isotope source (most commonly ^{60}Co). The problem with these methods of administering radiation is that they don't deliver their dose to just the cancer cells. Damage to surrounding cells can be quite significant. Over the years, there have been some inventive engineering solutions to this problem, most of which involve a rotating radiation source; this allows for the largest dose to be delivered at the point of intersection of the different beam directions, thus minimizing surrounding tissue damage [1].

2. Hadron Therapy

The alternative to more common radiation therapies being developed by particle physics laboratories around the world is known as hadron therapy. Hadron therapy is the use of subatomic particles composed of quarks to treat tumors.

Most hadron therapies exhibit distinctly different energy distributions through matter than photon radiotherapy. They possess a feature, known as a Bragg peak, made evident by plotting their dose against distance into tissue, known as a Bragg curve (Figure 1). Bragg curves can be used to show where the highest dose of radiation will be delivered, and are thus used in radiotherapy to assist in calculating the desired position and exact energy of the radiation being administered (Figure 1). The

curves are named after Sir William Henry Bragg, who along with his son William Lawrence Bragg, studied such data curves during their development of X-ray spectroscopy in the early 20th century.

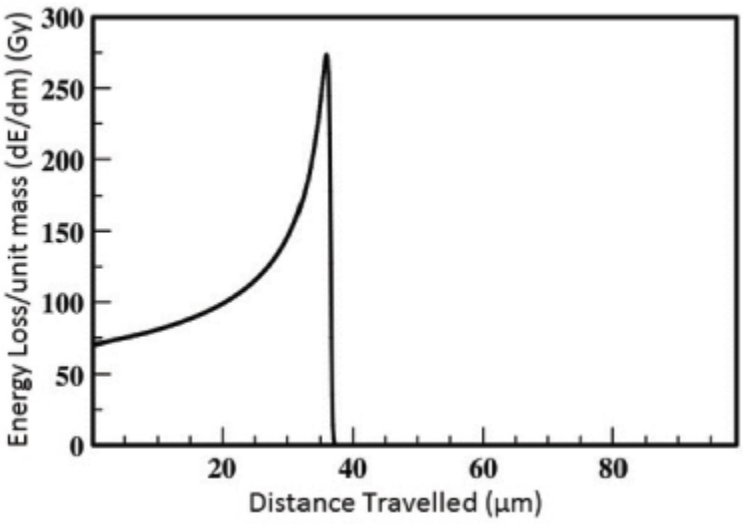

Figure 1 - A typical particle Bragg curve showing the loss of energy (dE/dx), or dose, as a function of distance travelled in water [2]

The peak in the Bragg curve comes about due to Coulombic interactions between the ion particle beam and the atoms in the matter being penetrated. As the ions interact, the particles in the incoming beam have their velocities decreased by the interacting electric forces. This loss in kinetic energy is converted directly into a photon (eq. (1)), giving rise to its radioactivity. This is known as *bremsstrahlung*, or breaking radiation. The lost kinetic energy is converted directly into photons:

$$m\,(v_2 - v_1) = E_2 \; - \; E_1 = h\,f \qquad (1)$$

As the particles slow down, their interaction cross section, and thus the probability that they will have further interactions with the surrounding matter, increases (eq. (2)). The relationship between the differential cross section of an interaction, and the kinetic energy of the incoming particle can be derived to be [3]:

$$\frac{d\sigma}{d\Omega} = \frac{1}{T^2}\left(\frac{Z_1 Z_2 e^2}{16\pi\varepsilon_0}\right)^2 \left(\frac{1}{\sin\left(\frac{\Theta}{2}\right)}\right)^4 \qquad (2)$$

where $d\sigma/d\Omega$ is the differential cross section of interaction, T is the kinetic energy, given by $T = ½\, mv^2$ for non-relativistic particles where m is the mass of the particle and v is its velocity, Z is the atomic number of the particles involved, e is the electron charge (1.6022×10^{-19} C), ε_0 is the permittivity of free space (8.85×10^{-12} F/m), and Θ is the angle of deflection.

Note the inverse relation of the cross section to the square of the kinetic energy (eq. (2)); this gives rise to the characteristic shape of the Bragg curve.

As the differential cross-section increases with decreased velocity, the incoming particles lose further kinetic energy as radiation, which leads to an exponential increase in energy lost to the surrounding tissue (eq. (2)). This exponential increase in interactions and energy losses gives the Bragg peak its characteristic exponential shape. Eventually, the particle will lose all of its kinetic energy, and this gives rise to the sharp cut-off point present on the Bragg curve of many hadrons (Figure 1).

The idea of using hadrons such as fast moving protons was first suggested just after the Second World War [4]. The most common form of hadron therapy is the use of accelerated proton beams directed at the tumor site to irradiate. Theoretically, the use of proton beams would allow for a maximum dose of radiation to be delivered at a specific point within the patient, and cause little to no permanent damage to surrounding tissue.

Proton beam therapy is already in use in cancer treatment centers across the world, however the facilities where such procedures are carried out are rare; only 54 such treatment centers capable of providing proton therapy exist worldwide, some of which have yet to begin treating patients.

This idea of using ion beams for cancer treatment is promising. There are, however, more effective ways in which the physics can be manipulated to augment treatment effectivity and lower the risk of excess damage further still. One such method is to increase the amount of energy available to be lost

as *bremsstrahlung*. This can be achieved by increasing the initial kinetic energy of protons. However, this would increase the penetration depth, and the target may be missed. A solution to this issue is offered by heavy ion beam therapy [5]. This is the use of heavier ions (usually carbon) in place of protons. Increasing the mass of the ions leads to an increase in the kinetic energy when these are accelerated to similar velocities as the protons, thus leading to an increase in the amount of energy available to transfer to surrounding tissue.

Carbon ions have similar characteristic Bragg curves to protons, exhibiting a much larger peak (up to 60% larger) just before coming to rest (Figure 2). A small *'tail'* present in carbon ion curves can be noted. This is known as the fragmentation tail (Figure 3) [6]. This is due to collisions of the carbon ions and target nuclei breaking into smaller radioactive particles, and contributing to the total dose [7].

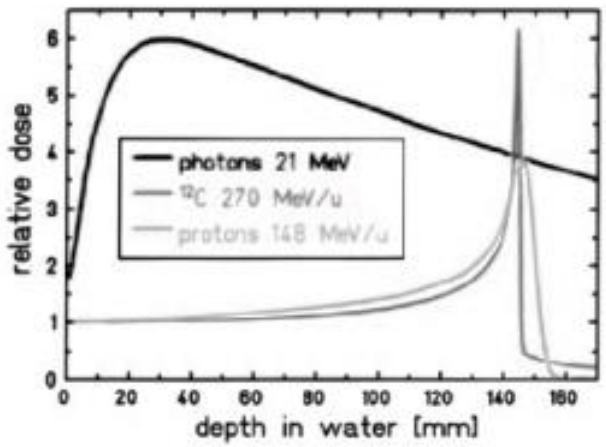

Figure 2 - Comparison of proton and C-ion beam Bragg curves to conventional photon therapy [8,9]

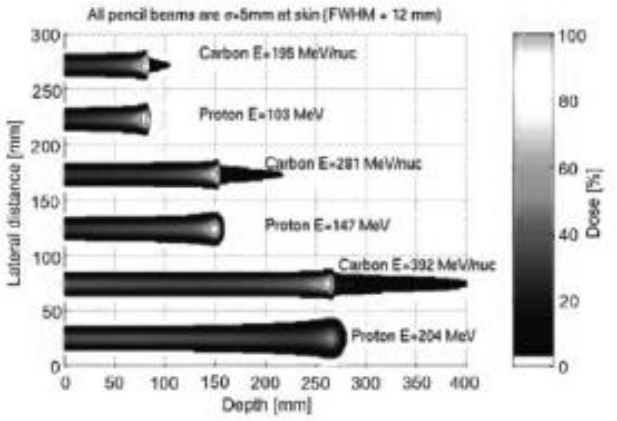

Figure 3 - Dose distribution comparison of proton and carbon ion beams. Note the fragmentation and increased dose at peak for the carbon beams [6]

Antiprotons are the antimatter counterpart of protons. This means that these particles share the same characteristics (for example the same mass), except for an opposite charge. Antimatter particles annihilate with their matter counterparts by liberating the energy corresponding to their respective masses. Thus, energy deposition consists of two components: stopping energy corresponding to the complete loss of kinetic energy until coming to rest (according to Bethe-Bloch), which is shared by protons, antiprotons and other particles, and annihilation energy, which is an exclusive feature of antimatter particles and will be discussed below. The stopping energies, however, are given for a specific kinetic energy and range and thus have to be compared using the same values for different particles. As for other particle beams, there are certain characteristics which differ from the clinically more common photon beams. These include the beam profile, which forms a Bragg peak, and the secondary particles or fragments which play a role in the biological effects and will be elaborated on. Antiprotons are interesting as a possible future modality in radiation therapy for the following reasons: when fast antiprotons penetrate matter, protons and antiprotons have near identical stopping powers and exhibit equal radiobiology well before the Bragg-peak. But when the antiprotons come to rest at the Bragg-peak, they annihilate, releasing almost 2 GeV per antiproton–proton annihilation. Most of this energy is carried away by energetic pions, but the Bragg-peak of the antiprotons is still

locally augmented with ~ 20 – 30 MeV per antiproton. Apart from the gain in physical dose, an increased relative biological effect also has been observed, which can be explained by the fact that some of the secondary particles from the antiproton annihilation exhibit high-LET properties. Finally, the weakly interacting energetic pions, which are leaving the target volume, may provide a real time feedback on the exact location of the annihilation peak. When fast antiprotons penetrate matter, they have the same stopping power as protons. The amount of primary particle loss is only slightly larger for antiprotons when compared with protons, and is less than that of carbon ions [10]. As the antiproton comes to rest, it will preferably be captured by a high-Z nucleus. For a polystyrene target ~ 99% of the antiprotons will therefore annihilate on a carbon nucleus, whereas the rest will annihilate with a hydrogen nucleus [11]. When captured by the target atoms, the antiproton will immediately spiral towards the nucleus and annihilate on its surface. This annihilation process releases 1.88 GeV corresponding to twice the rest-mass of the proton and the energy release is converted on average into 4 or 5 pions [12, 13]. The pions created are π+ and π^- particles, as well as π^0. The π^0 meson is highly unstable and decays instantaneously into high energy gamma-rays with roughly 70 – 300 MeV [12]. Due to the solid angle covered by the nucleus, 1 or 2 of the charged pions are most likely penetrating the nucleus inducing an intranuclear cascade, causing the nucleus to break into fragments [14–16]. Charged fragments have a very short range in the target and will deposit their kinetic energy in the immediate vicinity of the annihilation vertex. Also, we expect that some of these fragments will exhibit a high-LET and are responsible for an increase in biological effectiveness of antiproton annihilation compared to protons stopping in the target. Antiprotons annihilating on particles heavier than protons will also produce neutrons which will have a larger range and will lead to a certain level of background radiation. This needs to be studied carefully in the context of validating antiprotons for radiotherapy applications. The total energy deposited locally by these particles has been estimated by Gray and Kalogeropoulos using Monte Carlo calculations [17] to be 30 MeV per antiproton, which has been confirmed experimentally by Sullivan [18] who used a continuous beam of antiprotons from

the Low Energy Antiproton Ring (LEAR) at CERN and standard ionization chambers. This energy represents an increase of the physical dose deposition in the Bragg-peak by roughly a factor of 2, when compared to protons. In addition to this augmentation of the physical dose the secondary particles also cause the antiproton beam to have different radiobiological properties in the peak region.

A biomedical application of antimatter which is relatively widespread is positron emission tomography, which involves detecting the 511 keV photons characteristically emitted when a positron and its counterpart, the electron, annihilate. The annihilation energy of an antiproton and a proton on the other hand is much higher, amounting to 1.88 GeV. This energy is distributed among a variety of annihilation particles which either emerge from the annihilation itself or from reactions with nearby atoms. The most important groups of particles are charged and uncharged pions (together around 80% of the energy), neutrons, photons, heavy charged particles (ions of various nuclear charge and mass) and a small amount of other particles such as electrons, kaons and neutrinos [17, 19]. Pions and kaons belong to the family of mesons, which are hadrons (like protons and neutrons), but do only consist of two instead of three quarks. They have a mass, but are short-lived. In contrast, neutrinos are leptons, practically massless and hardly interacting with other matter. This variety of particles can further be discriminated by half-lives interaction patterns etc. However, it is important to note that the major biological effects in the target are due to the heavy particles with their high linear energy transfer (LET), although the exact composition of these particles is unknown [20, 21]. Most other particles leave the body without further interactions. Some particles, however, do interact in the body outside the target. In this regard, special attention has to be paid to neutrons, because of their relatively high biological effectiveness [22, 23]. When considering the diversity of the annihilation products, it is important to know how much energy will be deposited locally, i.e., in the target volume. The estimations for this proportion varied between less than 30 MeV [16] and up to150 MeV [17]. The latest experimental data and simulations point toward 30MeV being deposited in the immediate vicinity of the annihilation [19]. This amount of energy increases with increasing field size, due to

more secondary particles coming to rest within this increased radius; on the other hand, increasing field sizes also increase the amount of secondary particles coming to rest in other parts of the body, thereby increasing the dose halo [19].

When slowing down and coming to rest, the antiprotons eventually annihilate on a matter particle — the higher the mass, the more probable this event is [20]. The depth of the majority of the annihilation events, i.e., the length of the distance in the body, is subject to the energy of the antiproton beam and can be delineated very sharply, forming a Bragg peak. The depth-dose curve in water showed the antiproton Bragg peak being two fold higher compared to a proton beam of the same size and energy while at the same time showing only a slight elevation along the entry region [24]. A spread-out Bragg peak (SOBP) can be formed by variation of the beam energy, thereby covering a potential target volume.

When spreading out the beam, a number of parameters change. As mentioned above, the number of secondary particles increases, which is also the reason for the dose halo and the lateral penumbra to increase. In addition, it is known from other particles that when broadening the peak or modulation width, the difference in the RBE between peak and plateau (i.e., entrance region) will be reduced [19, 25, 26]. However, for antiprotons the interactions between RBE, LET and beam physics and the influence of changes on the dose distribution and the biological effects are only poorly characterized so far. Considerations regarding potential radiobiological advantages of antiprotons were primarily based on the increased energy deposition and on the heavy, high LET particles causing damage in the immediate vicinity of the annihilation point; a low oxygen enhancement ratio has also been attributed [27], but stands without experimental evidence. Due to the challenges in dosimetry, RBE values could only be estimated partly using values calculated through simulations and after implementing a quantity, defined as the ratio of fluences rather than doses, thereby dispensing of the need to assess the absolute dose [28]. When making several assumptions, this allows an estimate of the RBE, because fluence and dose are directly proportional. Following this approach, the RBE estimate for

antiprotons in a 2.5 mm SOBP for a 46.7 MeV pulsed beam was reported to be 2.25 [28], with a peak-to-plateau dose ratio of 4, both values roughly twice as high as for protons. The afore-mentioned assumptions were first that the antiproton RBE in the plateau (i.e., the in-flight RBE) is equal to that of protons [29, 30] and therefore 1 [31] and second that the Monte Carlo simulation of the antiproton dose ratio is accurate enough. However, the LET influences the RBE and therefore also has to be addressed. This explains that once the LET was known, RBE values from other experiments had to be re-evaluated. For the Bragg peak, the LET has recently been found to be around 19 keV/μm [29]; it has been indicated that the RBE in the plateau can be assumed to be around 1.2 – 1.3, instead of the 1 originally expected. This means the RBE in the peak region, which is expressed in relationto the RBE in the plateau region also had to be re-estimated: instead of 2.25 expected so far [28], it might rather be 2.7 – 3.0 (again, for very small SOBPs) [29]. The accuracy of the estimates for the RBE values may be improved when the plans to re-evaluate all experiments done so far is put into effect [32].

First proposals for possible clinical indications were rather wide; the antiproton was seen as a particle superior to all others [17]. With increasing knowledge and understanding, the settings with possible advantages for antiprotons narrowed. In 2008, the possible role for antiprotons in radiotherapy has been seen as potentially useful for three groups of patients [20]: First, re-irradiation of patients with local failure after radiotherapy (taking advantage of a potential sparing of surrounding tissues). Second, small tumors with organs-at-risk directly neighboring (potentially improved sparing again). Third, therapy-resistant subvolumes in a tumor (using the unique radiobiological properties of antiprotons with their high RBE). Two years later, a comparison of antiproton, proton and carbon ion treatment plans in a water phantom with a PTV of $4 \times 4 \times 4$ cm^3 surrounded by $1 \times 1 \times 1$ cm^3 volumes of interest was published [33]. This simulation revealed that antiprotons have the highest peak-to-plateau ratio, but do deposit dose beyond the PTV; carbon ions in comparison have a longer tail, whereas protons deliver no dose at all beyond the PTV. Outside the PTV, the dose from antiprotons

spreads isotropically whereas carbon ions contain a directional component. Antiprotons deliver the lowest dose to the entrance region and the highest to the PTV, thereby increasing the dose lateral and beyond the PTV. The mean dose to the whole phantom (excluding the PTV) for the antiproton beam has been calculated to be 3.6% of the PTV dose, thus being twice as high as for the other particles. This study used laterally modulated fields to improve the target coverage. In contrast, Paganetti et al. [19] had used flat and also larger fields (10×10 cm^2), which deliver worse results in terms of target coverage and normal tissue sparing. Since the dose volume histograms for antiprotons and carbon ions only differed slightly in the treatment plan comparison by Bassler et al.[33], it has been concluded that only big differences in the RBE could compensate for the larger lateral penumbra and the background dose faced when using antiprotons.

An important question arising in the studies is which field or target size can be seen as clinically realistic. Most studies performed so far concentrated on narrow beams. However, the resulting, very small field sizes tend to underestimate the normal tissue dose due to secondary particles—a problem, which is much more pronounced for antiprotons than for protons [19]. Even when stating that clinically relevant target volumes in antiproton radiotherapy will rarely reach the dimensions of one liter, it has to be kept in mind that at least some increase in background dose has to be expected. A general limitation of most of the studies performed so far and reported here is the simplistic setting with cubic water phantoms; this clearly has to be kept in mind when interpreting the results.

The summarized results can lead to the conclusion that antiprotons probably offer advantages only in those cases where the normal tissue in the entrance region is of special importance. In this context, it has to be highlighted that a typical peak-to-plateau ratio for a proton beam is around 5 – 6, for a carbon ion beam similar, maybe higher (depending on beam line physics, RBE and other factors) and for an antiproton beam of the same energy around 9 –10 [24, 34, 35] (Figure 4). This ratio is very favorable for antiprotons, but it worsens with increasing beam energy [19, 36]. Many other characteristics also depend on the beam energy used: Besides the range and the peak-to-plateau ratio, this is also true for the in-flight annihilation probability, the secondary particle spectrum [34] and

radiobiological effects [33]. Recently, energy and intensity modulated treatment plans based on Monte Carlo simulations have been shown to be feasible for antiprotons [37].

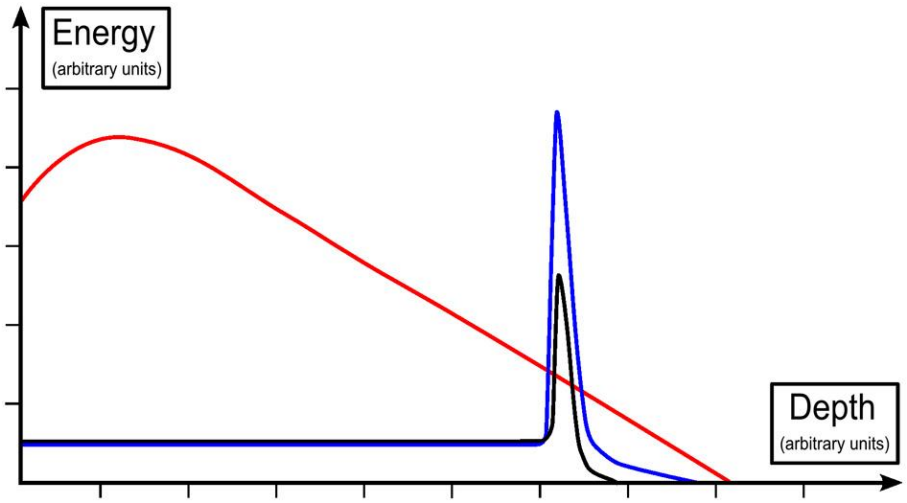

Figure 4 - Schematic display of depth dose profiles of a photon (red), proton (black) and antiproton beam (blue), with deposited energy expressed relative to the plateau region [40]

A possible modification of antiproton radiotherapy has been proposed by Shmatov [38]: When heavy elements such as Uranium-238 or Thorium-232 are brought into a tumor, the biologically effective dose administered with a given antiproton radiotherapy may be increased by 10% or more. This is explained with an increased amount of short-range particles due to the annihilation with the heavy elements and may be also a reduced annihilation probability with other nuclei. However, these are only hypotheses lacking experimental data and not taking into account clinical complexities such as the effective introduction of the named substances into the tumor and toxicities potentially associated with it. In addition, irradiating heavier elements has also been suggested to lead to a smearing of the irradiated spot due to an increased neutron yield [39].

There are a number of more exotic treatments under development in medical particle accelerator facilities. Hadrons consist of two main groups, baryons and mesons. Baryons are composed of three quarks (although theories suggest that exotic baryons consisting of up to nine quarks could exist [41]

and make up most of the baryonic matter in the universe. Mesons are composed of one quark and one antiquark. The use of mesons for radiotherapy has similar advantages to the baryonic therapies discussed above. π-meson (or pion) beam therapy has been suggested as an alternative [42, 43] but is not a common treatment for cancer. The pions decay producing a number of secondary particles that in turn decay, releasing a much higher dose of radiation than from just the initial decay. Depending on the type of pion beam used in treatment, a number of decay routes are possible.

The simplest decay is that of neutral pions (π^0) into two photons [44]. π^0 are composed of either an up and an antiup quark, or a down and an antidown quark. They thus have extremely short lifetimes (approximately 0.1 fs [45]). However, this can prove problematic as a treatment, as there is currently no way of directly controlling a π^0 beam in a magnetic field due to its lack of electronic charge.

The more viable option, and also more complex, is charged pion decay. Charged pions have much longer lifetimes (approximately 26 ns [46]) and can be easily accelerated, due to their charge. The primary mode of pion decay is a purely leptonic decay into a muon, and a muon antineutrino via a W^+ boson (Figure 5). Such particles can also decay into electrons and electron antineutrinos, or positrons and electron neutrinos, depending on the charge conservation. This decay is, however, far less probable.

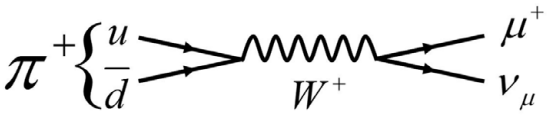

Figure 5 – Lowest order Feynman diagram showing the decay of the π^+- meson into muons and neutrinos via a W^+ boson. The decay for the π^-- meson is similar, only with opposite charge conservation.

Both the positive and negative pions can decay via this route, however the π- has the additional option of binding to a nucleus in the tumour tissue, and interacting to the nucleus that captured it [44]. If the nucleus in question is hydrogen, the π^- can interact with the proton, and produce a π^0 and a neutron, or a neutron and a photon [43], as shown in eqs. (3, 4):

$$\pi^- + p \rightarrow \pi^0 + n \rightarrow n + 2\gamma$$

$$\pi^- + p \rightarrow n + y$$

(3, 4)

The elementary muons produced in pion decay can also contribute to the total radiation dose. As the muons decay, the binding energy of the muon is released as radiation.

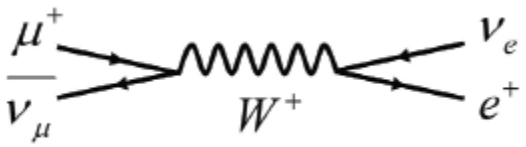

Figure 6 - Lowest order Feynman diagram of positive muon (μ^+) decay into a muon antineutrino, a positron and an electron neutrino via a W^+ boson.

The exact dynamics of this decay change depending on what flavour of muon decays (Figure 6) (eqs. (5, 6)). When a μ^+ decays, it decays into a muon antineutrino, a positron and an electron neutrino via a W^+ boson (eq. (5)), releasing energy in the process. Further energy is released upon the subsequent positron-electron annihilation.

$$\mu^+ \rightarrow e^+ + \nu_e + \overline{\nu}_\mu + hf$$

(5)

However, if a μ^- is present, the μ^- can displace an electron in an atom, and bind to the nucleus, creating a form of exotic matter known as a muonic atom. The captured μ^- can then relax to the ground state from its excited state, releasing photons before decaying into a muon neutrino, an electron and electron antineutrino via a W^- boson (eq. (6)), along with more photons.

$$\mu^- \rightarrow e^- + \overline{\nu}_e + \nu_\mu + hf$$

(6)

If the μ^- is captured by a hydrogen nucleus in the tumour, further irradiation is caused by electron capture (or inverse β-decay) and the emission of a 5.1 MeV neutron [43].

It should be noted that muon beam therapy could also be used as a cancer treatment, however, as such particles are technically not hadrons, they are simply discussed as a side-product of other hadron therapies in this review.

The most effective treatment in radiation oncology would need to be a combination of the methods previously discussed. Antiproton radiotherapy is a method that combines the dose distribution of proton therapy with the large energy releases of the other decay methods [20, 47]. Protons and antiprotons share similar interaction characteristics before the Bragg peak, exhibiting similar radiobiology and differential interaction cross-section. The difference between their radioactivity occurs when antiprotons reach the Bragg peak. As the antiproton comes to rest, proton-antiproton annihilation occurs. This is a complex process, involving some clean quark-antiquark annihilation, with the formation of new pions and kaons from the rearrangement of the remaining quarks of the collision (along with the gluon interactions forming strange quarks for kaon formation). The pions

that are created would then decay as described above, releasing more energy, and the subsequent muon decay would release further energy still.

The decay of additional radioactive side-products of proton-antiproton annihilation increases the effective dose at the Bragg peak by about 20-30 MeV per antiproton (on average) when compared to the proton Bragg peak [20]. This treatment combines the increased effectiveness of heavy ion hadron therapy at the target site without the increased dose before the Bragg peak [28]. The fragmentation tail is still observed due to the multitude of additional radioactive shrapnel particles ejected in the annihilation.

While hadron therapy has many benefits over conventional radiotherapy, it is important to note some of its disadvantages. Studies have shown that while proton therapy can give far more targeted results by way of delivering the majority of radiation at the target site, the more powerful heavy-ion and antiproton therapies have drawbacks that become more noticeable when put to practical use. The fragmentation tail caused by secondary particles begins to become a serious issue when doses are applied across the entire tumour, causing a halo of damage to surrounding healthy cells [19]. The peak-to-plateau ratio as one of the major advantages of the antiproton beam properties is still a highly valuable feature. However, the lateral penumbra and increased dose halo compared to other particle beams reduce the applicability of antiprotons to very few possible indications. There may be clinical settings — especially when the normal tissue in the entrance region of the beam is highly radiosensitive — where antiproton radiotherapy offers special advantages. Possible clinical constellations include the treatment of recurrences, when the normal tissue has already received the maximum tolerable dose, and the dose in the entry channel has to be minimized. These settings have to be further analyzed by generating and comparing treatment plans and the respective dose distributions, based on assessments of the physical qualities of antiprotons in comparison with the different beam types available so far. In addition, the possibilities for real-time dose range verification offer a new feature in contrast to other particle beams which might attract more attention in the future.

Other open questions exist regarding the role of secondary neutrons, which should be investigated following the appropriate ICRP protocols. Also, the biological properties of the antiproton beam have to be further characterized considering different cell lines and target sizes, as well as the effects of the medium and long-range secondary particles. In particular, the RBE — which depends on correct dosimetry —has to receive further attention. This has to be seen as a prerequisite for meaningful treatment planning studies, because as long as the biological properties are not validated, antiproton treatment planning cannot be performed. But only then will it be possible to think about *in vivo* experiments, which in turn require new facilities providing adequate fluence rates. Finally, the most important quantity is the ratio of the biologically effective dose in the target volume and the biologically effective dose to the normal tissue. This in turn has to be evaluated carefully in terms of cell killing (e.g., in the tumor) and of induction of secondary tumors (in the normal tissue). Hence, there are still many open questions which need to be addressed by future research.

3. References

[1] D.A. Warrel, T.M. Cox , J.D. Firth, *The Oxford Textbook of Medicine*, (5 ed.), Oxford University Press, 1983

[2] J.J. Bevilacqua, *Peer J.*, 2015:1143

[3] E. Rutherford, *Philos. Mag.* 1911:6(21):669

[4] R.R. Wilson, *Radiobiology*, 1946:47(5):487

[5] C.D. Schlaff, A. Krauze, A. Belard, J.J. O'Connell, K.A. Camphausen, *Radiation Oncology*, 2014:9(88)

[6] H. Suit, T. Delaney, S. Goldberg, H. Paganetti, B. Clasie, L. Gerweck, K.O. Niemer, E. Hall, J. Flanz, J. Hallman, A. Trofimov, *Radiotherapy and Oncology*, 2010:95:3

[7] U. Amaldi, G. Kraft, *Europhysics News*, 2005, 36(4), 114

[8] E. Fokas, G. Kraft, G. An, H. Egenh, R. Cabillic, *Biochimica et Biophysica Acta - Reviews on*

Cancer. 2009:1796(2):216

[9] O. Ronan, *Trinity Student Scientific Review*, Vol. 2, 2016

[10] N. Bassler, M. Holzscheiter, H. Knudsen, Low Energy Antiproton Physics-LEAP ’05, vol. CP796 of AIP Conference Proceedings. American Institute of Physics, 2005; pp. 423–430.

[11] L.I. Ponomarev, *Annu Rev Nucl Sci* 1973:395

[12] Jr Agnew, E. Lewis, T. Elioff, B. Fowler William, L. Lander Richard, M. Powell Wilson M, E. Segre`, *Phys Rev* 1960:1371

[13] M. Inokuti, *Nucl Tracks Radiat Meas* 1989;16:115

[14] J. Cugnon, S. Wycech, J. Jastrzebski,P. Lubinski, *Phys Rev C* 2001;63:27301

[15] W. Markiel, H. Daniel, T. von Egidy, F.J. Hartmann, P. Hofmann, W. Kanert, *Nuclear Physics A* 1988;485:445

[16] D. Polster, D. Hilscher, H. Rossne, T. von Egidy, F.J. Harmann, J. Hoffmann, *Phys Rev C* 1995;51:1167

[17] L. Gray, T.E. Kalogeropoulos, *Radiat Res* 1984:246

[18] A.H. Sullivan, *Phys Med Biol* 1985;30:1297

[19] H. Paganetti, M. Goitein, K. Parodi, *Radiother Oncol*. 2010; 95:79

[20] N. Bassler, J. Alsner, G. Beyer, J.J. DeMarco, M. Doser, D. Hajdukovic, *Radiother. Oncol*. 2008:86:14

[21] H.V. Knudsen, M.H. Holzscheiter, N. Bassler, J. Alsner, G. Beyer, J.J. DeMarco, *Nucl. Instrum. Methods B* 2008: 266:530

[22] E.J. Hall *Radiother.Oncol*. 2006:81:231

[23] N. Bassler, H. Knudsen, S.P. Moller, J.B. Petersen, D. Rahbek, U.I. Uggerhoj, *Nucl. Instrum. Methods B* 2006:251:269

[24] N. Bassler, M.H. Holzscheiter, O. Jäkel, H.V. Knudsen, S. Kovacevic, *Phys. Med Biol.* 2008:53:793

[25] M.R. Raju, E. Bain, S.G. Carpenter, R.A. Cox, J.B. Robertson, *Br. J. Radiol.* 1978: 51:704

[26] M.R. Raju, H.I. Amols, E. Bain, S.G. Carpenter, R.A. Cox, J.B. Robertson, *Br. J. Radiol.* 1978:51:712

[27] H.R. Withers, S.P. Lee, W. McBride, T.D. Solberg, J.J. DeMarco, N. Agazaryan, *Radiother. Oncol.* 2002:64:S93

[28] M.H. Holzscheiter, N. Bassler, N. Agazaryan, G. Beyer, E. Blackmore, J.J. DeMarco, *Radiother. Oncol*. 2006:81:233

[29] N. Bassler, M. Holzscheiter, *Acta Oncol.* 2009:48:223

[30] P. Weber, *AD-4/ACE: Antiproton Cell Experiment. SSRMP Annual Scientific Meeting (Basel) Abstracts and Proceedings* 2009:27:30.

[31] B.G. Wouters, G.K.Y. Lam, U. Oelfke, K. Gardey, R.E. Durand, L.D. Skarsgard, *Radiat Res.* 1996:146:159

[32] M. Holzscheiter, J. Alsner, A. Angelopoulos, N. Bassler, G. Beyer, R. Boll, *Status Report for Experiment AD* 2013

[33] N. Bassler, I. Kantemiris, P. Karaiskos, J. Engelke, M.H. Holzscheiter, J.B. Petersen, *Radiother. Oncol*. 2010:95:87

[34] S.M. Handley, S. Ahmad, *J. Xray Sci. Technol.* 2011:19:34

[35] H. Suit, T. DeLaney, S. Goldberg, H. Paganetti, B.Clasie, L. Gerweck, *Radiother. Oncol.* 2010:95:3

[36] N. Agazaryan, J.J. DeMarco, S.P. Lee, J.B. Smathers, T.D. Solberg, H.R. Withers, *Radiother. Oncol.* 2002:64:S52

[37] B. Fahimian, J. DeMarco, R.L. Keyes, S. Luan, M. Zankl, M. Holzscheiter, *Med. Phys*. 2009: 36:2758

[38] M.L. Shmatov, *Tech. Phys. Lett.* 2008:34:335

[39] M. Kossov, *IEEE Trans. Nucl. Sci.* 2005:52:2832

[40] M. Bittner, A.-L. Grosu, N.Wiedenmann, J.J.Wilkens, *Frontiers in Physics* 2014:1:1

[41] R. Aaji *Phys. Rev. Lett*. 2015:115(7):072001

[42] M.R. Raju, *Negative pion beams for radiotherapy*, Symposium on Pion and Proton Radioherapy, Batavia, Illinois., 1971.

[43] N.V. Mokhovy, A.V. Ginneken, *Muons versus Hadrons for Radiotherapy*, Proceedings of the Particle Accelerator Conference, New York, 1999

[44] F.M. Khan, *The Physics of Radiation Therapy*, Philadelphia, PA: Lippincott Williams & Wilkins, 2012

[45] K. Von Dardel, G. Dekkers, D. Mermod, R. Vanputten, J.D. Vivargent, M. Weber, G. Winter, *Physics Letters*. 1963:4:5

[46] D.H. Perkins, *Particle Astrophysics*, Oxford University Press, 2003

[47] J.N. Kavanagh, F.J. Currell, D.J. Timson, K.I. Savage, D.J. Richard, S.J. McMahon, O. Hartley, G.A.P. Cirrone, F. Romano, K.M. Prise, N. Bassler, M. Holzscheiter, G. Schettino, *Scientific Reports* 2013:3:1770